PHYSICAL AGING EFFECTS ON THE COMPRESSIVE LINEAR VISCOELASTIC CREEP OF IM7/K3B COMPOSITE

by David R. Veazie and Thomas S. Gates
Langley Research Center, Hampton, Virginia

ABSTRACT — An experimental study was undertaken to establish the viscoelastic behavior of IM7/K3B composite in compression at elevated temperature. Creep compliance, strain recovery and the effects of physical aging on the time dependent response was measured for uniaxial loading at several isothermal conditions below the glass transition temperature (T_g). The IM7/K3B composite is a graphite reinforced thermoplastic polyimide with a T_g of approximately 240^{o}C. In a composite, the two matrix dominated compliance terms associated with time dependent behavior occur in the transverse and shear directions. Linear viscoelasticity was used to characterize the creep/recovery behavior and superposition techniques were used to establish the physical aging related material constants. Creep strain was converted to compliance and measured as a function of test time and aging time. Results included creep compliance master curves, physical aging shift factors and shift rates. The description of the unique experimental techniques required for compressive testing is also given.

Introduction

Advanced polymer matrix composites (PMC's) are desirable for structural materials in diverse applications such as aircraft, civil infrastructure and biomedical implants because of their improved strength-to-weight and stiffness-to-weight ratios. The development of analytical and experimental tools to aid in the study of composite durability is the impetus for intensive design and development studies at NASA and major industry based airframe developers [1].

A possible disadvantage of polymer-based composites is that the physical and mechanical properties of the matrix often change significantly over time due to exposure to elevated temperatures and environmental factors. This problem has resulted in an extensive research initiative to develop comprehensive material property characterization techniques and analytical modeling methods aimed at predicting the long term mechanical response of polymer matrix composites at elevated temperatures. The ultimate goal is to develop accurate analytical models and accelerated test methods needed to engineer advanced polymer matrix composites to ensure long-term structural integrity over the design life-time.

This paper presents unique experimental techniques and apparatus used to measure the viscoelastic behavior of PMC’s in compression at elevated temperatures. Isothermal, constant load, creep compliance measurements were performed on the matrix dominated transverse and in-plane shear behavior of IM7/K3B in compression. Linear viscoelasticity was used to characterize the creep and superposition techniques were used to establish the physical aging related material constants. The resulting creep compliance master curves, physical aging shift factors and shift rates can be used as input data to a viscoelastic creep compliance procedure to establish time dependent behavior and predict long term response. The observed differences in the time

dependent behavior in the transverse and in-plane shear directions along with the effects of elevated temperature are discussed.

Physical Aging Characterization

The main focus of this research is one aspect of long-term polymer matrix composite viscoelastic behavior: *physical aging*. Physical aging is a process, occurring below the glass transition temperature (T_g), where the macromolecules gradually change their packing in order to approach the equilibrium free volume state [2]. The gradual approach towards equilibrium affects the mechanical properties of the polymer, often resulting in a material that is stiffer and more brittle, so that the compliance is decreased (or the modulus increased) over what one would have expected in a viscoelastic material without aging. In terms of free volume theory, one can visualize that as the free volume decreases towards its equilibrium values, the mobility of chain segments is hindered, giving rise to a stiffer response. Aging is a characteristic of the glassy state and is found in all polymer glasses, as thoroughly documented by Struik [3]. The effects of physical aging continue until the material reaches volume equilibrium. The time required to reach volume equilibrium depends on the aging temperature. During this time the mechanical properties may change significantly [4,5].

Several experimental studies have illustrated that the matrix dominated composite properties of continuous fiber reinforced PMC's, namely the shear and transverse response, are affected by physical aging in a manner similar to pure polymers [4,5,6,7]. Struik [3] showed that it was possible to isolate the physical aging process in polymers from other behaviors by performing isothermal creep compliance tests and using superposition techniques to establish the aging

related material constants. An illustration of the creep and recovery tests for determining aging effects is shown in Figure 1. In these tests, the specimen is initially quenched from above T_g to a temperature below T_g. The time the material exists below its glass transition is referred to as the aging time, t_e. As aging time progresses, a series of short (in comparison to the elapsed aging time) creep segments of duration t_i are run to extract the momentary creep compliance of the material. In this figure, the compressive (negative) strain is shown in the first quadrant (positive) for reader clarity. Throughout this study, negative strain was converted to positive strain for use in existing data reduction routines that were created for positive strain. The momentary creep compliance of the material, $S(t)$, can be described with a three parameter fit model, first proposed for linear viscoelastic glass by Kohlrausch [8],

$$S(t) = S_o e^{(t/\tau)^{\beta}} \qquad (1)$$

where S_o is the initial compliance, β is a curve shape parameter, t is time, and τ is the relaxation time.

In nearly all cases of aging of polymers and PMC's, it is possible to bring the momentary creep curves measured at different aging times into superposition through a horizontal shift. This result is akin to the well known time-temperature superposition principle [9]. The aging time shift factor, a_{t_e}, is defined as the horizontal distance required to shift a compliance curve to coincide with a reference compliance curve. If the aging time shift factor is plotted as a function of aging time on a double-log scale, it is found to map a straight line with a slope of μ. The shift rate, μ,

$$\mu = - \frac{d(\log a_{t_e})}{d(\log t_e)} \tag{2}$$

usually has values on the order of unity and can be considered to be a material constant. Thus, a series of creep and recovery tests (as in Figure 1) can be used to experimentally determine the value of the shift rate, μ, for any given material.

Since the momentary creep curves collapse through horizontal shifting on the log scale, the only parameter which changes as a function of aging time is the relaxation time. The momentary material properties must then vary with aging time according to

$$S(t) = S_o e^{(t/\tau(t_e))^{\beta}}, \tag{3}$$

where

$$\tau(t_e) = \tau(t_{e[ref]}) / a_{t_e} , \tag{4}$$

$t_{e[ref]}$ is the reference aging time, $a_{t_{e[ref]}} = 1$ and the shift factor is defined as

$$a_{t_e} = \left(\frac{t_{e[ref]}}{t_e} \right)^{\mu} . \tag{5}$$

Thus to describe the momentary creep compliance at any aging time, the parameters needed are the initial compliance S_o, the curve shape parameter β, the shift rate μ, and the relaxation time τ at a reference aging time $t_{e[ref]}$ [1].

It is the intent of this work to establish unique experimental techniques to accurately measure the compressive creep strain and recovery strain as a function of test time and aging time for the

time dependent response of fiber reinforced polyimide composites. Resulting compressive creep compliance master curves, physical aging shift factors and shift rates for inclusion in Struik's effective time theory are used to model the physical aging effects in the composite.

Test Materials and Specimen Configuration

The material system chosen for this study was a continuous carbon fiber reinforced thermoplastic polyimide fabricated by DuPont and designated IM7/K3B. The fiber, IM7, was an intermediate modulus carbon fiber manufactured by Hercules. The unaged T_g in the composite as measured by Dynamic Mechanical Analyzer (DMA) G'' peak was 240°C. Change in the T_g from the unaged condition over extended aging times was measured by industrial studies and found to remain within 3°C over 10,000 hours of isothermal aging at 170°C [10]. For this study, it was therefore assumed that chemical aging of the composite would not occur and the T_g would remain constant over the duration of the tests.

Rectangular test specimens similar to those described in ASTM Specification D3039-76 measuring 20.32 cm. by 2.54 cm., and consisting of 12 or 8 plys of approximately 0.0135 cm. thickness, were cut from laminated panels. The in-plane transverse (S_{22}) and in-plane shear (S_{66}) creep compliance data came from unidirectional 12-ply $[90]_{12}$ and angle-ply 8-ply $[\pm 45]_{2s}$ specimens, respectively, where the subscripts *22* and *66* represent, respectively, the material coordinate perpendicular to the fiber and the shear directions. Test were not conducted to determine the other compliance components (S_{11}, S_{12}) due to their time-independent behavior. Three replicates were used at each test temperature. Although all the specimens came from the same material lot, many of the replicate specimens were cut from different panels.

Test Equipment

All of the creep tests were performed in convection ovens equipped with digital controllers. Copper-constantan (ANSI symbol ″T″) thermocouples located near the test section provided feedback for the oven controller and were used with a scanning thermocouple thermometer to monitor the test temperatures. Thermal apparent strain was corrected for by using the compensating gage technique [11]. A diagram of the experimental setup is shown in Figure 2.

A uniaxial constant load was applied through a dead-weight cantilever arm tester that reacted at a point outside the test chamber. A unique apparatus shown in Figure 3 was constructed to allow a tensile creep test frame to be used for application of a compressive load. The compressive creep apparatus consisted of two rigid frames connected by steel rods running through linear bearings. The apparatus was designed such that the two frames could move in-plane relative to each other when a tensile load was applied. To minimize friction between the contacting surfaces, the steel rods were polished smooth and the linear bearings were lubricated with heat-resistant dry graphite lubricant.

The specimen was positioned in the center of the apparatus and end loaded by the convergence of the two inner rigid fixtures. Lightweight grips incorporating straight saw tooth faces were fixed to the specimen ends to prevent slipping. Each grip consisted of two halves held together by pins for accurate alignment. The contact surfaces between the grip ends and the rigid fixtures were precision ground to transfer the load uniformly to the specimen. The gripped specimen was held in alignment by small pins attached to brackets mounted on the inner rigid fixtures.

To ensure stable compression, the specimen was supported from column buckling by lightweight knife edge guides as shown in figure 4. The guides were mounted on the specimen however since they did not connect to the grips, they did not carry any of the applied axial load. The knife blades were easily adjustable to allow for minimal contact with the specimen surface and various specimen thickness. Column buckling was checked during loading by longitudinally aligned back-to-back strain gages, which would show a lack of parity in strain if simple bending occurred. A sample plot of the strain parity from back-to-back strain gages is shown in Figure 5.

During the unloaded or recovery segments, the two inner rigid fixtures were separated from the specimen grips by applying a slight compressive force from the creep frame lever arm. This recovery procedure, however, left the lightweight upper grip and the knife edge guides to remain fixed to the specimen and possibly hinder complete strain recovery. In order to verify whether or not the weight of the upper grip and the knife edge guides had an effect on complete recovery, a benchmark run was performed for the case of an unloaded specimen at test temperature. The run showed that the lightweight upper grip and the knife edge guides had no effect on the creep or recovery strain on the specimen. This unloading process therefore provided for virtually unconstrained recovery while allowing the test chamber to remain closed during the entire test sequence.

Strain in the gage section was measured with high temperature foil strain gages applied in the center of the specimen. Micro-Measurement WK-000-250BG-350 gages bonded with the M-Bond 600 gage adhesive and 220^{o}C solder were used. The M-Bond 600 was cured at 120^{o}C for two hours. This combination of gage and adhesive seemed to minimize the problems associated with coefficient of thermal expansion (CTE) mismatch to the composite and gage/adhesive creep.

Proper selection of this gage type and adhesive gave CTE match and stability at elevated temperatures.

Stress was calculated based upon the applied load and the specimen cross-section before testing. For the $[90]_{12}$ specimens, the average measurement of two back-to-back gages, aligned longitudinally, was used to compute (S_{22}). For the $[\pm 45]_{2s}$ specimens, the average measurement in each direction of four gages, two back-to-back aligned longitudinally and two back-to-back aligned transversely was used to compute (S_{66}). The compliance terms used in data reduction for these specimens are given as

$$S_{22}(t) = \frac{\varepsilon_x(t)}{\sigma_x}, \tag{6}$$

$$S_{66}(t) = \frac{2\varepsilon_x(t)[1-\varepsilon_y(t)/\varepsilon_x(t)]}{\sigma_x}, \tag{7}$$

where σ_x and ε_x is the stress and strain in the loading direction, respectively, and ε_y is the strain perpendicular to the load. Each gage formed a quarter-bridge circuit. Thermal strain compensation was accomplished during data reduction. Commercially available instrumentation provided bridge completion, excitation and signal conditioning. A personal computer equipped with a 12-bit A/D board converted and stored the high level analog output signal from the amplifiers.

Prior to testing, all specimens were dried for at least 24 hours at 110°C in a convection oven. Immediately after drying, the strain gage adhesive installation was subjected to a postcure segment by heating to 230°C for two hours. Following the postcure, the specimens were stored

inside a desiccator until the gages were actually wired at the start of testing. After each test sequence the specimens were visually inspected for matrix cracks along their edges with an optical microscope. These inspections revealed no apparent damage after the sequenced tests.

Experimental Procedures and Data Reduction

To explore the effects of physical aging on the creep properties, a well documented technique that measures the creep compliance as described in Struik [3] and depicted in Figure 1, was used for all tests. This procedure consisted of a sequence of creep and recovery tests using a constant applied load while the specimen isothermally ages.

All of the tests were conducted under isothermal conditions using monotonic compressive loads. The test temperatures selected for the study were 200^{o}, 208^{o}, 215^{o}, 220^{o}, 225^{o}, and 230^{o}C. These test temperatures actually exceed the expected use temperatures of the material, however they were selected to ensure that measurable aging occurred within the test period.

To ensure that all test specimens start the test sequence in the same unaged condition, a means of rejuvenating the specimen was required. Rejuvenation was accomplished by a procedure based upon work by Struik [3] and others who showed that physical aging is thermoreversible and the excursion above T_g prior to quenching effectively rejuvenates the material. In the current tests, the gauged specimen was heated to 250^{o}C (10^{o}C above T_g) for 30 minutes immediately before the start of any physical aging test sequence. During this period above T_g the material is more compliant than in its glassy state. Consequently, a support bar was fastened between the upper and lower grips of the vertically positioned specimen to prevent any shape alteration that might be

caused by the weight of the upper grip or the knife edge guides during rejuvenation. This support was easily removed following rejuvenation.

The method used to quench specimens from above T_g to the aging temperature varies between investigators, such as using liquid nitrogen or submersing in an ice-water bath [12,13]. A procedure by Sullivan [4] which utilized high-pressure air to quench the specimen was adopted for use in this study. This method provided the only practical means to quench the material when strain gages and wires are attached to the specimen. After reaching the test temperature during this rapid quench, the material is in an unaged condition and the aging time clock can be started. Temperature stabilization after quenching typically took less than three minutes.

The duration of each creep segment was 1/10th the duration of the prior total aging time. The aging times (time after quench) selected for starting each creep segment were 2, 4, 10, 24, 48, 72 and 96 hours. After each creep segment, the specimen was unloaded and allowed to recover until the start of the next creep test. To facilitate recovery, the specimen remained in the convection oven at temperature while being unloaded. The recovery times were long enough to allow for nearly complete strain recovery. However, to account for any remaining residual strain due to a lack of complete recovery, the strain measured in the creep segment was corrected by subtracting the extrapolated recovery strain from the prior creep curve.

For the creep tests, an applied stress level was chosen for each layup and used at all temperatures. Determination of the applied stress level within the linear viscoelastic range was made by checking that both Boltzman's superposition and proportionality conditions would be met at the highest temperature for a given layup. Given an initial state of stress σ' applied for a

time t and an additional stress σ'' applied at time t_1, Boltzman's superposition principle [9] states that:

$$\varepsilon\left[\sigma'(t)+\sigma''(t-t_1)\right]=\varepsilon\left[\sigma'(t)\right]+\varepsilon\left[\sigma''(t-t_1)\right]. \tag{8}$$

Therefore, Equation 8 implies that given creep data, superposition would allow the exact prediction of the subsequent recovery period so that

$$\varepsilon(t-t_1)=\sigma\left\{S(t)-S(t-t_1)\right\}, \tag{9}$$

where σ is the constant stress, t_1 is the time of load removal, and $S(t)$ is the creep compliance function. Compressive creep and creep/recovery data provided data for checking superposition.

Proportionality states that for an applied stress σ, the strain in a material at any other stress is found using:

$$\varepsilon\left[c\sigma(t)\right]=c\varepsilon\left[\sigma(t)\right] \quad \text{where } c = \text{constant.} \tag{10}$$

A proportionality check was performed by plotting isothermal, creep compliance versus test time for a specimen that was repeatedly rejuvenated, quenched and loaded at various stress levels. The supposed transition from linear to nonlinear behavior would be evident by the vertical separation of the compliance curves with increasing stress. These checks were made at the lowest and highest test temperatures thereby ensuring that the effects of applied stress were minimized for all temperatures and a linear assumption could be used in any model with assurance of reasonable accuracy.

Figure 6 provides an example of the curve fits used to characterize each sequenced creep compliance curve. The momentary sequenced creep/aging curves were collapsed through a horizontal (time) shift using the longest aging time curve as the reference curve. Figure 7 shows the collapsed curve from the data shown in Figure 6. In some cases, small vertical (compliance) shifts (as compared to the horizontal shifts in terms of the double-log scale plots) were also used in reduction of the IM7/K3B data. The sets of both horizontal shifted collapsed data and horizontal and vertical shifted collapsed data, known as momentary master curves, were fit with Equation 1. The parameters from this fit were termed the momentary master curve parameters for a given temperature.

The time shifts (*log a*) used to collapse the sequenced curves shown in Figure 6 were plotted versus log aging time and approximated through a linear fit, as shown in Figure 8. The slope of this shift factor versus aging time data is the shift rate μ.

Results and Discussion

The range of linear viscoelastic behavior was experimentally determined to satisfy the conditions of proportionality. Experiments were also conducted to assure that the linear Boltzman's superposition condition was met for all tests. Using the test and data reduction procedures outlined above, the short term sequenced creep compliance data for IM7/K3B was found as a function of aging time over a range of five temperatures. Isothermal momentary master curves for the transverse (S_{22}) and shear (S_{66})terms were generated to show the temperature dependency of short term creep compliance and the directional dependency of the PMC.

To evaluate the proportionality criteria, creep tests were run at 230°C and 225°C, representing the maximum test temperatures used for transverse and shear compliance respectively. The applied stress levels were between 3.56 MPa and 1.81 MPa for the transverse compliance proportionality tests and between 8.34 MPa and 5.59 MPa for the shear compliance proportionality tests. Coincidence of the transverse compliance curves in Figure 9 and the shear compliance curves in Figure 10 indicated that the different stress levels caused little variation in compliance on the log scale although there was some small trend in location of the curves in relation to the applied stress. Based upon these results and the fact that the same applied stress level was to be used at all temperatures, proportionality was met for all tests.

The strain history of a typical creep/recovery sequence for a $[\pm 45]_{2s}$ specimen is shown in Figure 11. The condition of linear Boltzman's superposition is assumed to be satisfied because of the good correlation between the predicted recovery strain from Equation 9 and the measured recovery strain. It was recognized that the assumption of linear viscoelastic behavior based upon these results might not be conclusive, however it was felt that deviations from linearity were small enough to confidently proceed with linear modeling. The final applied stress levels chosen for the creep tests were 2.68 MPa and 6.97 MPa for the transverse and shear tests, respectively.

Three replicate specimens were used over a range of five temperatures to generate the isothermal momentary master curves for transverse (S_{22}) and shear (S_{66}) terms. Table 1 provides the momentary master curves parameters (S_o, τ, β) found by fitting Equation 1 to the combined data sets from all replicates. It should be noted that even though only one set of momentary master curve parameters is given in Table 1, each of the replicate tests had their own shift rate (μ)

found through the procedures described previously. Therefore, the shift rate given in Table 1 is an average value. The standard deviation of μ is also provided in Table 1. The average shift rates are plotted versus test temperature in Figure 12 for the transverse and shear compliance. The data points in this figure were connected with a smooth curve to illustrate the trends. These tests show that the transverse direction shift rate falls continuously, while the shear shift rate is fairly level until 225^{o}C.

For comparison purposes, the resultant momentary master curves for each temperature which correspond to the data in Table 1 are plotted together in Figures 13 and 14 for the transverse and shear compliance, respectively. These master curves represent the sum of all the short term sequenced creep compliance data.

Concluding Remarks

A unique creep compression apparatus is proposed for studying viscoelastic behavior of composite specimens at elevated temperatures. The apparatus appears to provide a means for stable, consistent testing of thin coupon type test specimens. Column buckling was suppressed and localized instability was prevented through the use of support fixtures. The apparatus and associated experimental techniques presented in this study would provide the experimenter with the type of data necessary to make accurate comparisons between compressive and tensile viscoelastic/aging effects in thin composite members.

Linear viscoelastic behavior during creep compression can be assumed if sufficient testing is performed to confirm the validity of Boltzman's superposition principle and proportionality. Aside from the obvious sign differences from tensile creep testing, compressive testing can take

advantage of established procedures. Care must be taken however, to pick a stress level which gives linearity over the complete range of temperatures yet also provides enough creep strain to develop the compliance curves.

Time/temperature and time/aging time superposition techniques developed for characterizing physical aging during tensile creep work equally as well with compressive creep. Shifting and collapsing creep compliance curves was a straightforward process and lent itself well to the formation of master curves and the three parameter characterization. The momentary master curves show the clear temperature dependency of short term creep compliance. The ordering of the curves was as expected with the highest temperatures resulting in the highest creep compliance. The directional dependency of the PMC is also evident by noting the differences in the compliance between the transverse and shear tests.

Master curve parameters combined with aging shift rates, effective time theory, and lamination theory should allow for the prediction of long term compressive creep compliance behavior of thin composite laminates under elevated temperature. Verification of this will require long term data for a variety of laminates.

References

[1] Brinson, L. C. and Gates, T. S., "Effects of Physical Aging on Long-Term Creep of Polymers and Polymer Matrix Composites," INT. J. SOLIDS STRUCTURES, **32**, (6), 827-846, (1995).

[2] Kovacs, A. J., Stratton, R. A., and Ferry, J. D., "Dynamic Mechanical Properties of Polyvinyl Acetate in Shear in the Glass Transition Temperature Range," JOURNAL OF PHYS. CHEM., **67**, (1), 152-161, (1963).

[3] Struik, L. C. E., Physical Aging in Amorphous Polymers and Other Materials, Elsevier North-Holland Inc., New York, NY, (1978).

[4] Sullivan, J. L., "Creep and Physical Aging of Composites," COMPOSITE SCIENCE AND TECHNOLOGY, **39**, 207-232, (1990).

[5] Hastie, R. L. and Morris, D. H., "The Effect of Physical Aging on the Creep Response of a Thermoplastic Composite," ASTM STP 1174, C. E. Harris and T. S. Gates, Eds., Philadelphia, PA, 163-185, (1993).

[6] Gates, T. S., and Feldman, M., "Time-Dependent Behavior of a Graphite/Thermoplastic Composite and the Effects of Stress and Physical Aging," JOURNAL OF COMPOSITES TECHNOLOGY & RESEARCH, JCTRER, **17**, (1), 33-42, (1995).

[7] Sullivan, J. L., Blais, E. J., and Houston, D., "Physical Aging in the Creep Behavior of Thermosetting and Thermoplastic Composites," COMPOSITES SCIENCE AND TECHNOLOGY, **47**, 389-403, (1993).

[8] Kohlrausch, R., "Nachtrag uber die Elastische Nachwirkung beim Cocon- und Glasfaden, und die Hygroskopische Eigenschaft des Ersteren," POGG. ANN. PHYS., **72**, 393-425, (1847).

[9] Ferry, J. D., Viscoelastic Properties of Polymers, 3rd Edition, John Wiley and Sons, Inc., New York, NY, (1980).

[10] Feldman, M., and Gates, T. S., "Physical Aging Tests Above 200^{o}C," SOCIETY FOR EXPERIMENTAL MECHANICS' SPRING CONFERENCE, (May, 1994).

[11] Murry, W. M., and Miller, W. R., "The Bonded Electrical Resistance Strain Gage," Oxford University Press, New York, (1992).

[12] Booij, H. C., and Palmen, J. H. M., "Viscoelasticity of ABS Samples Differing in Thermal History," POLYMER ENGINEERING AND SCIENCE, **18**, (10), 781-787, (1978).

[13] Kong, E. S. W., "Sub-T_g Annealing Studies of Advanced Epoxy-Matrix Graphite-Fiber-Reinforced Composites," JOURNAL OF APPLIED PHYSICS, **52**, (10), 5921-5925, (1981).

List of Figures

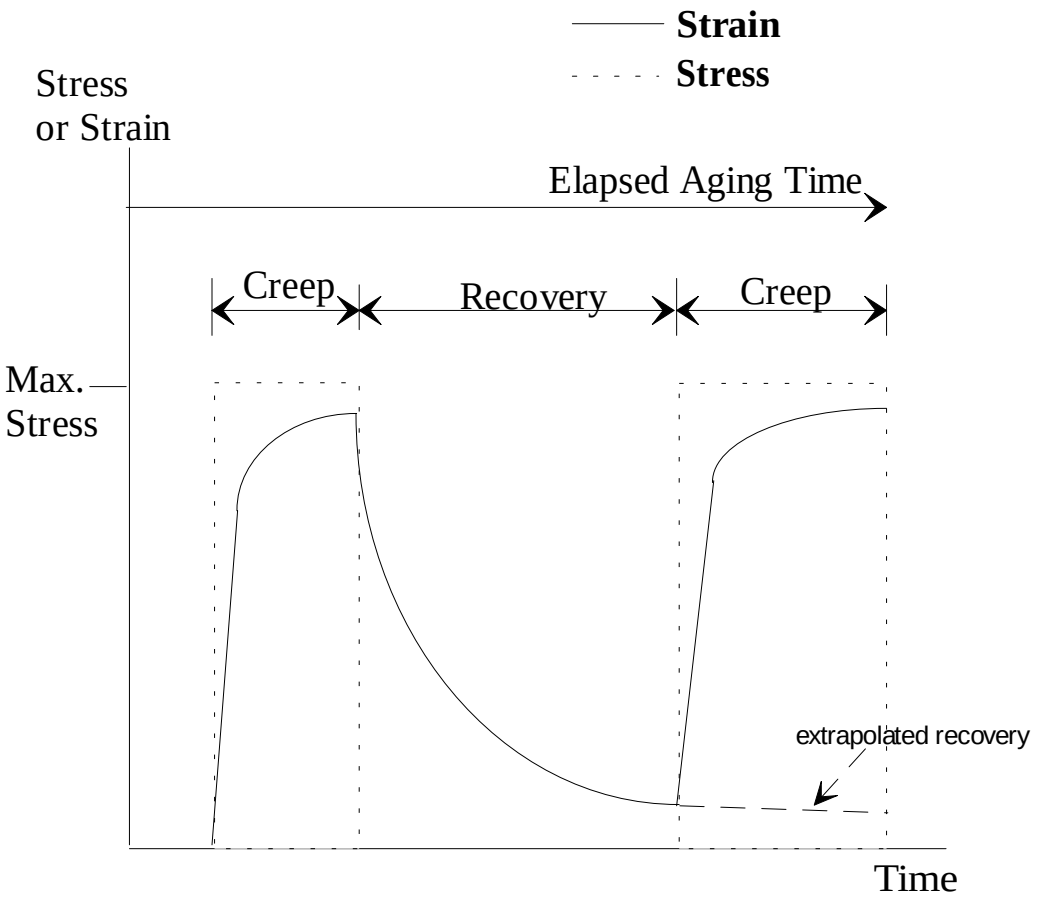

Fig. 1. Sequenced creep compliance test procedures.

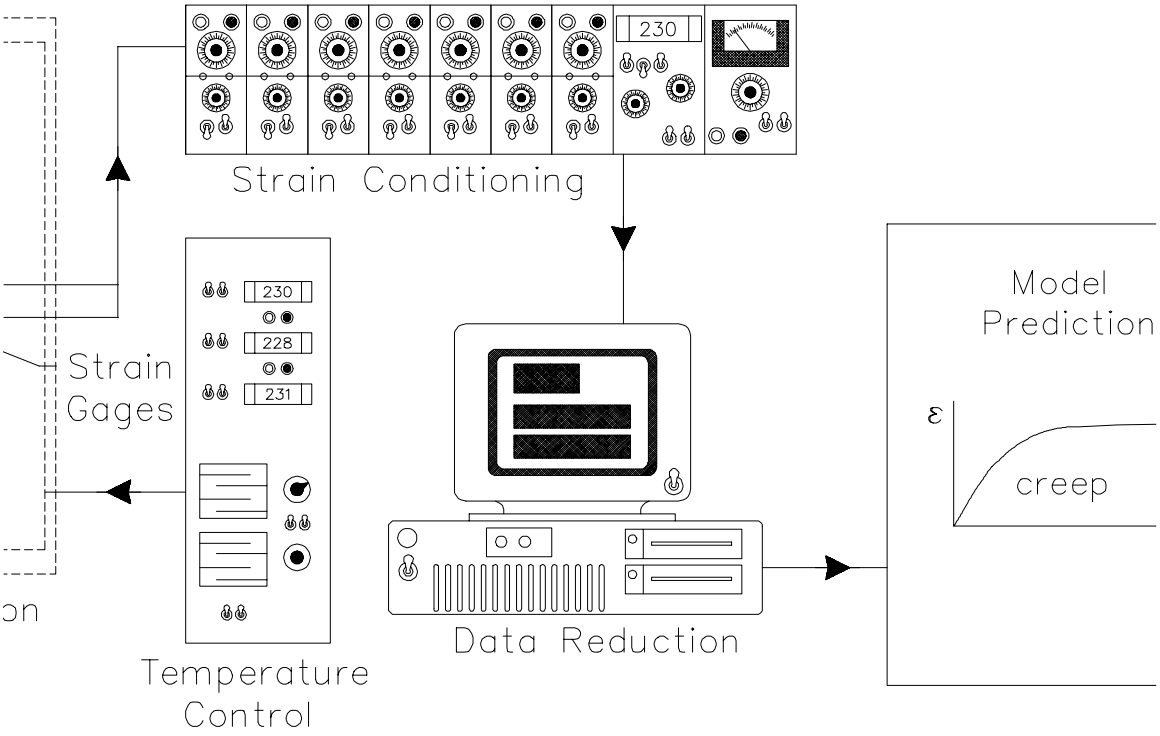

Fig. 2. Diagram of experimental setup.

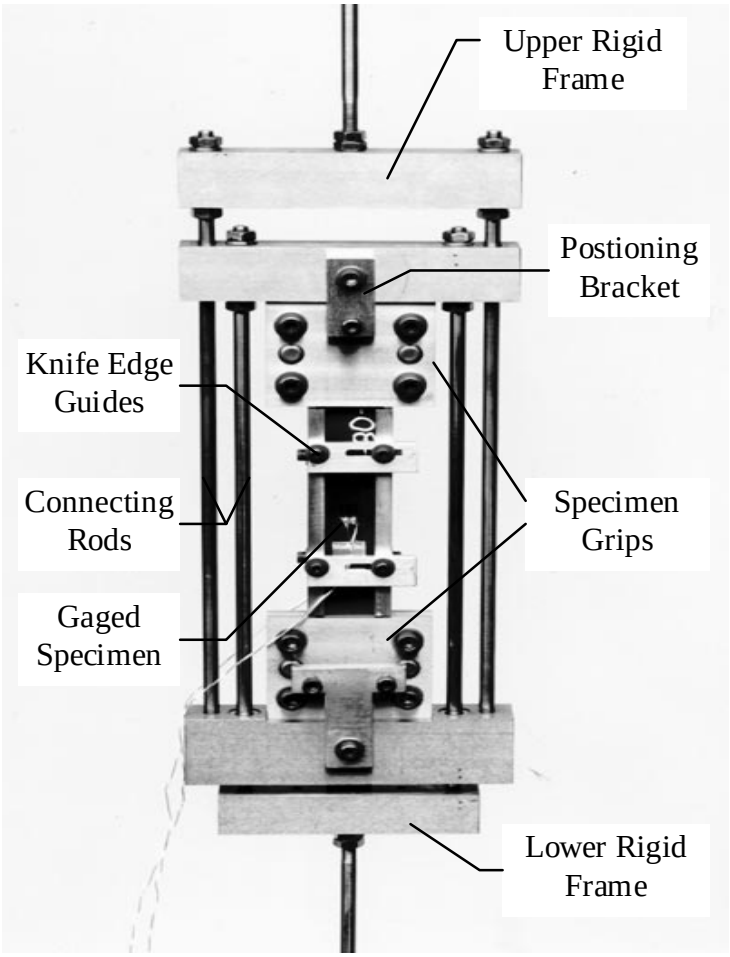

Fig. 3. Compressive creep apparatus with test specimen.

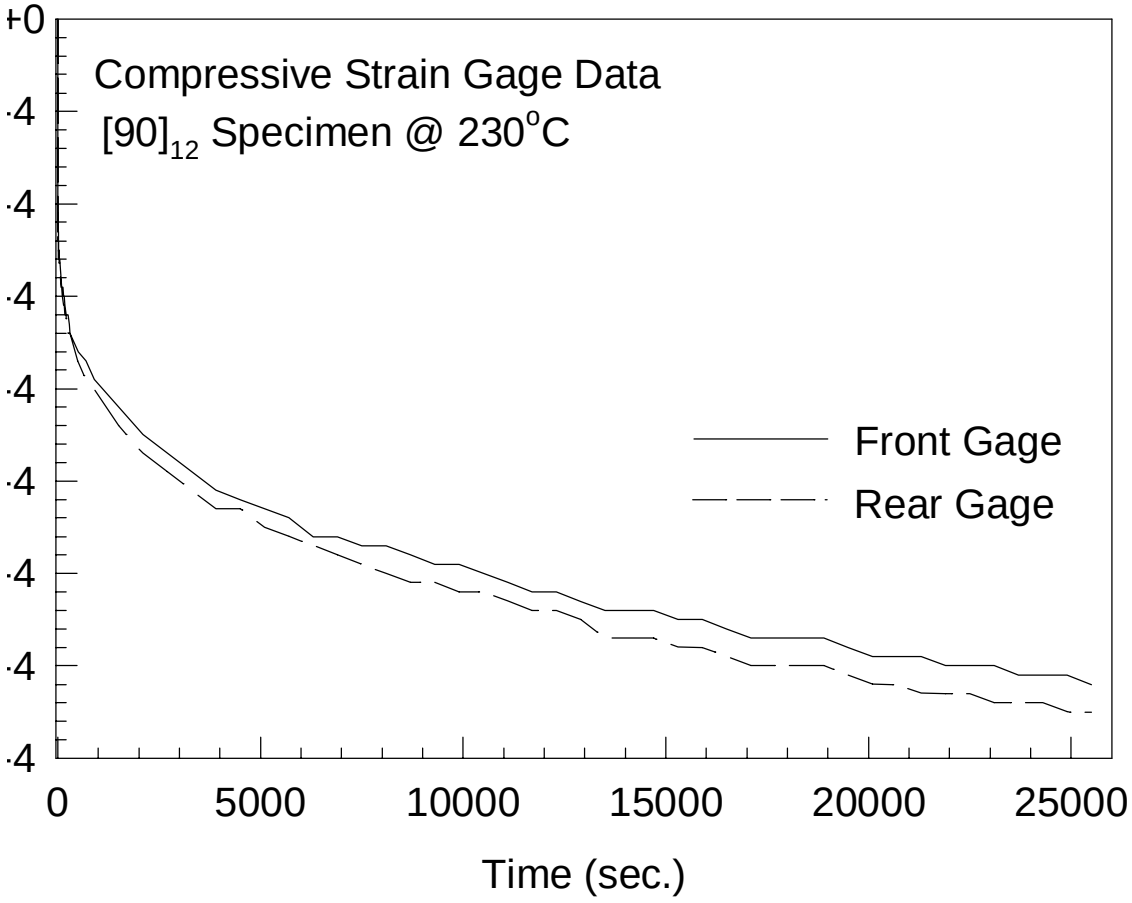

Fig. 5. Strain parity from back-to-back strain gages.

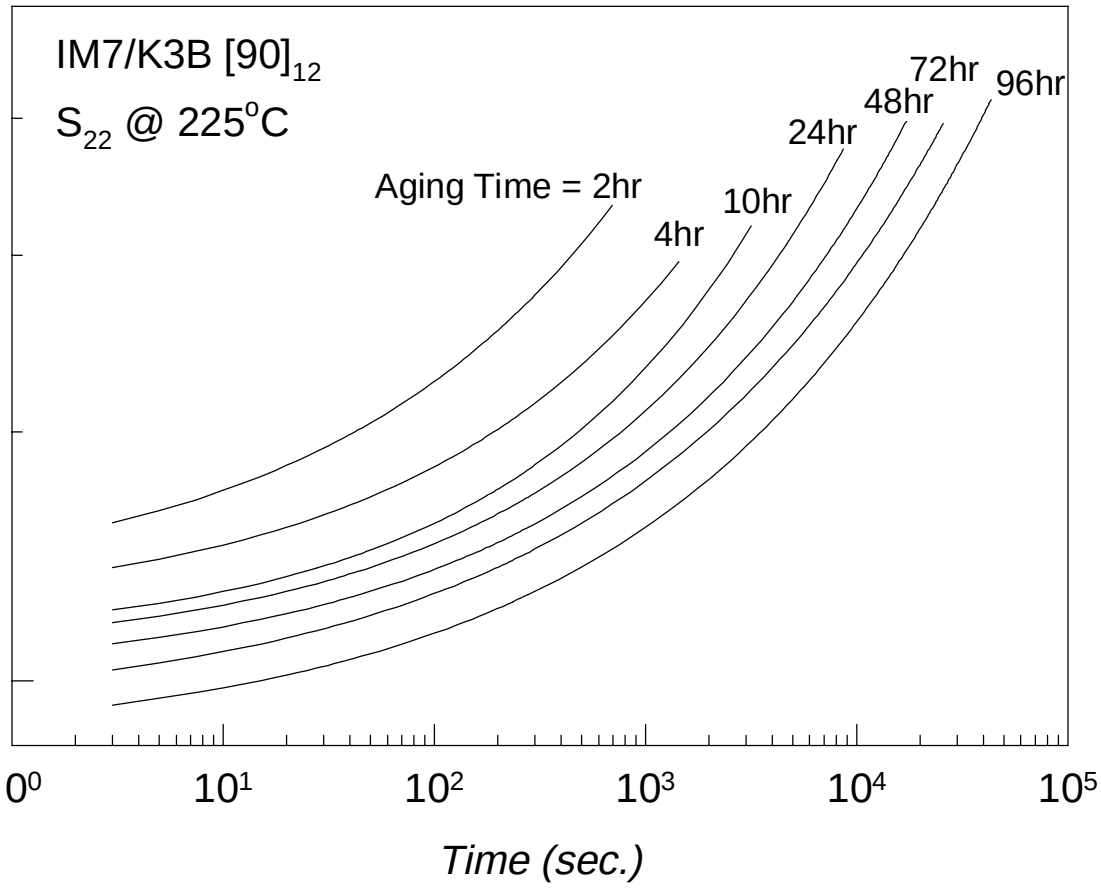

Fig. 6. Typical transverse compliance momentary curves.

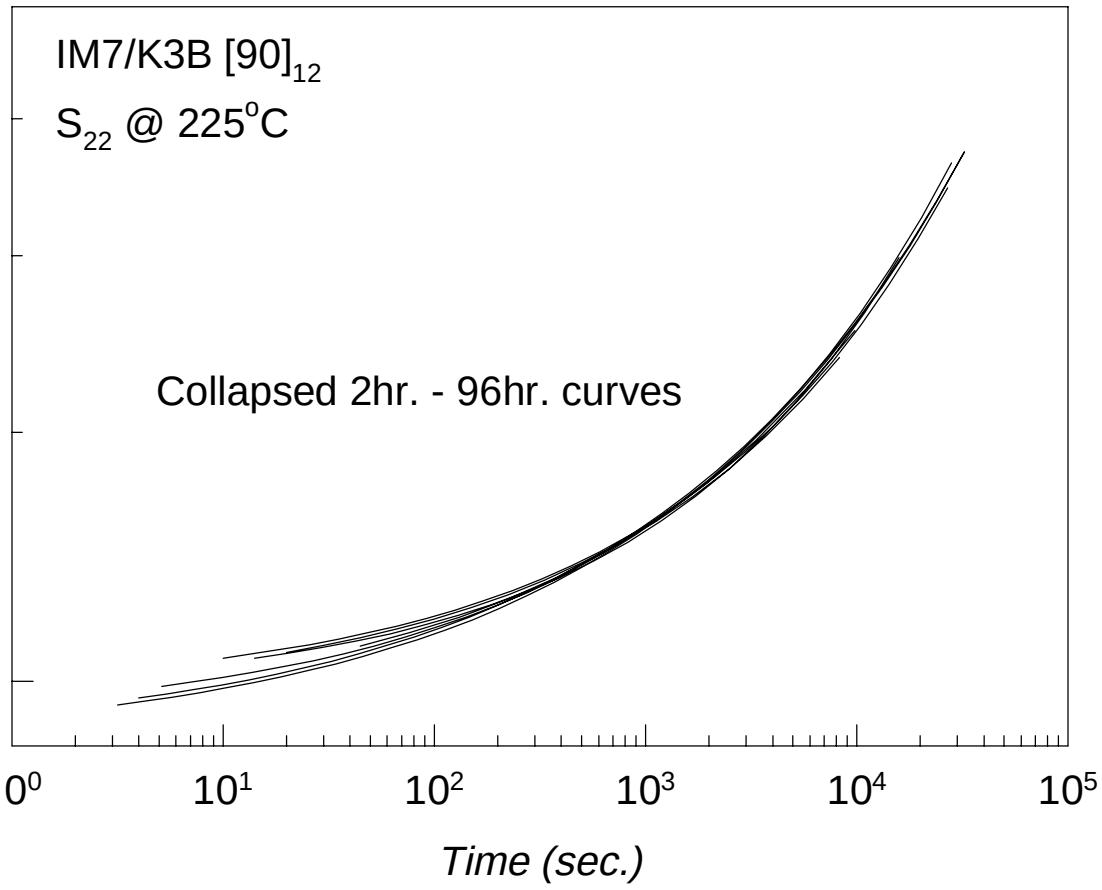

Fig. 7. Typical momentary creep compliance during aging.

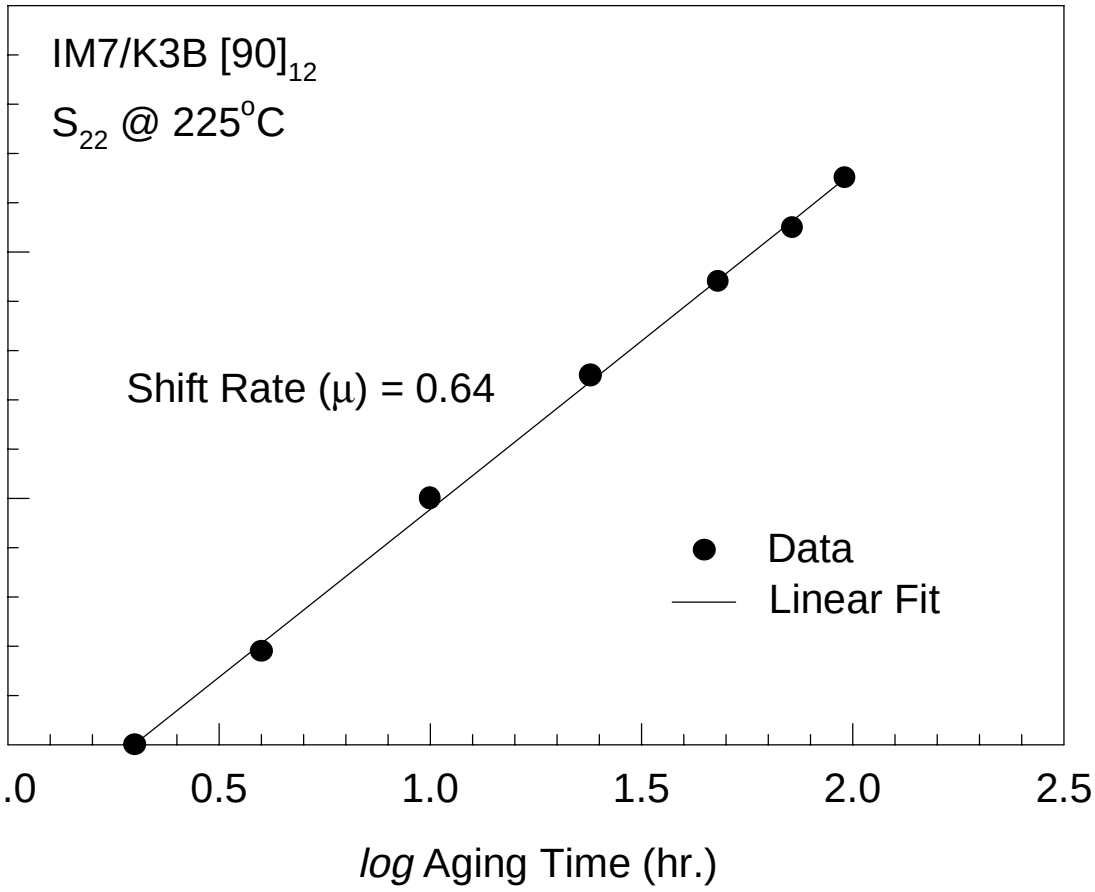

Fig. 8. Typical aging shift factor as a function of aging time.

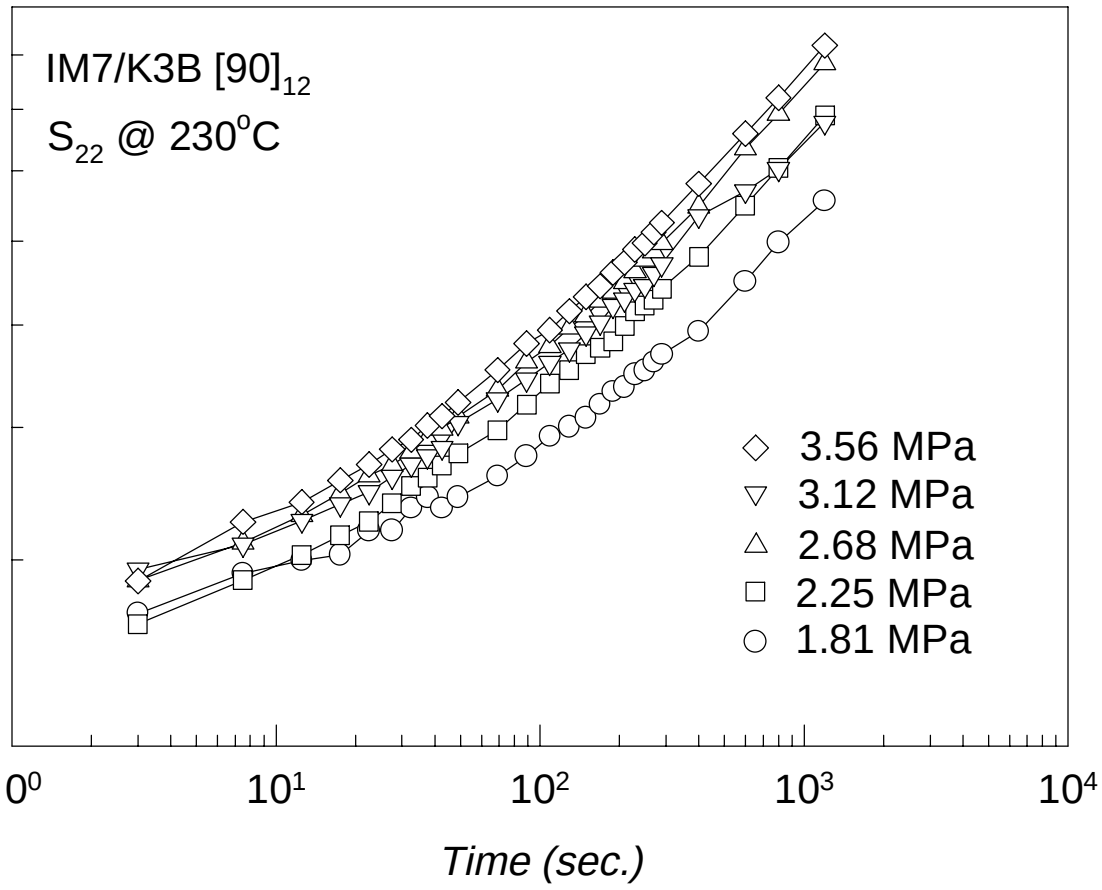

Fig. 9. Transverse compliance proportionality check.

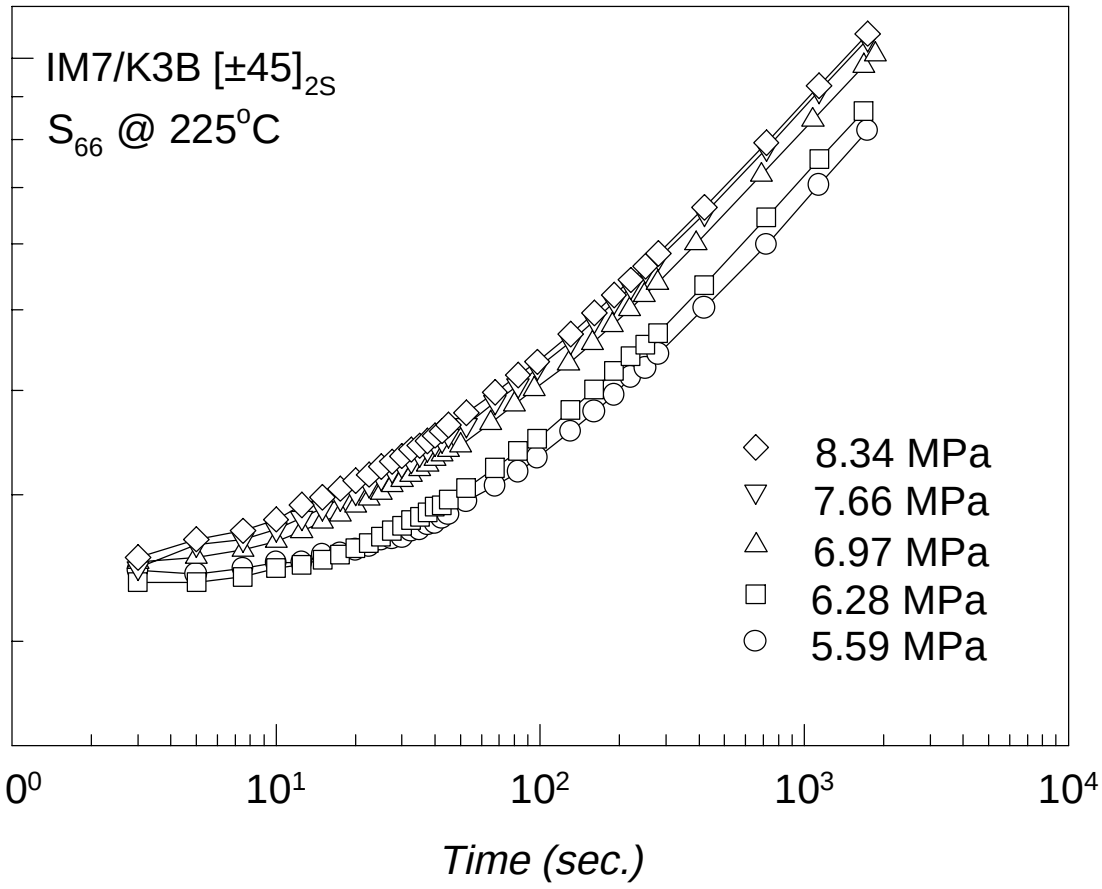

Fig. 10. Shear compliance proportionality check.

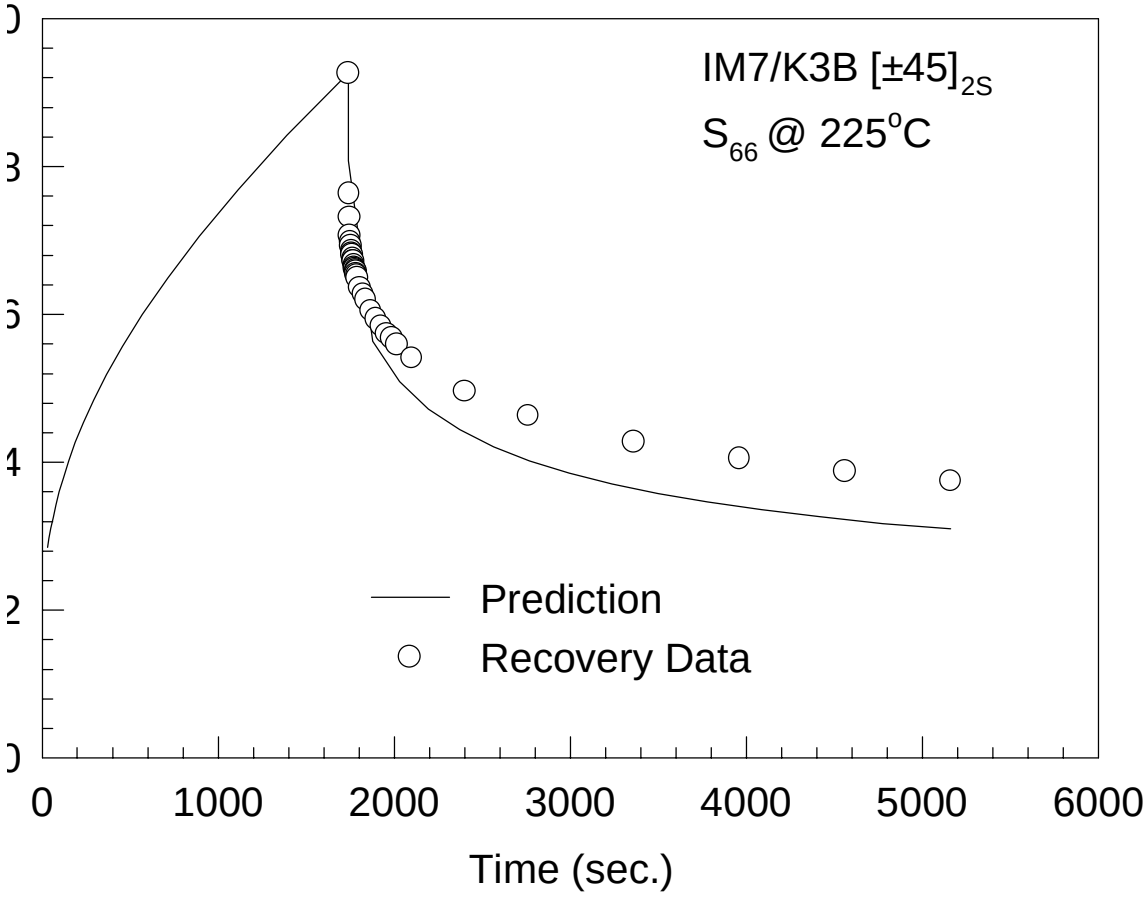

Fig. 11. Linear superposition creep/recovery sequence.

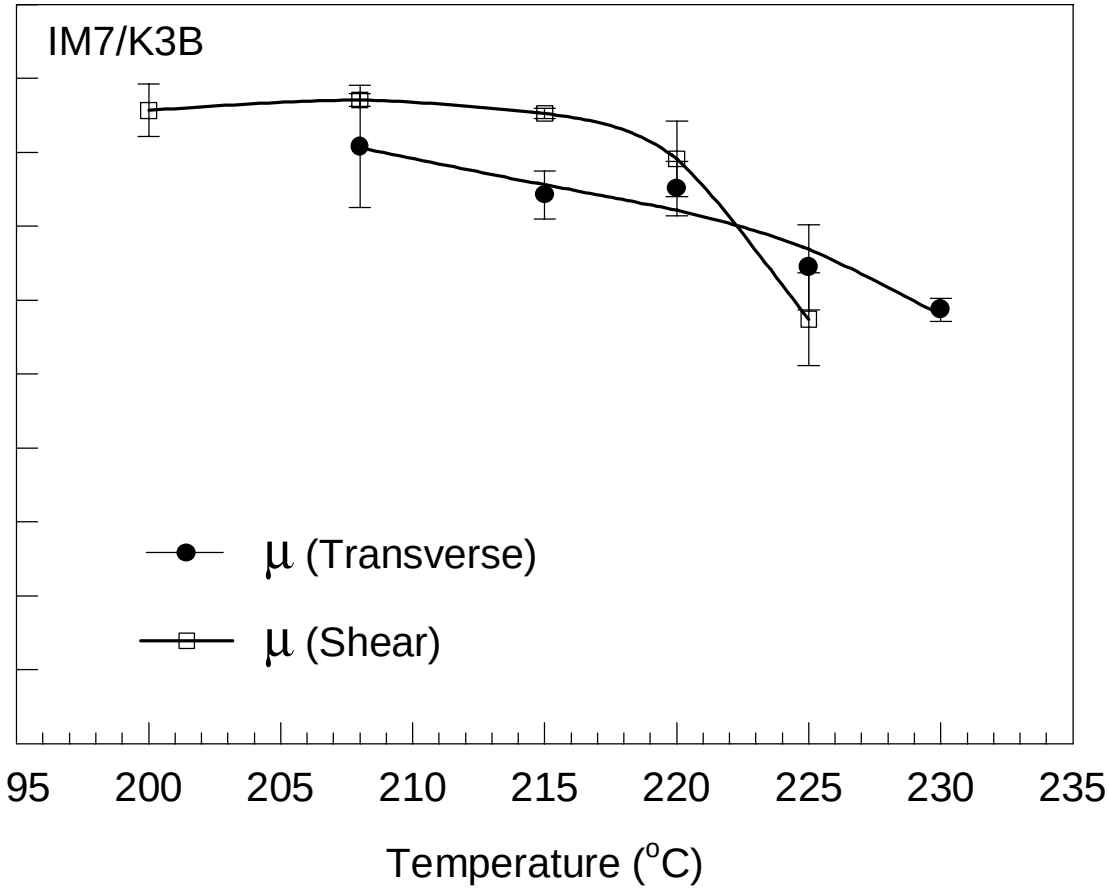

Fig. 12. Transverse and shear compliance shift rate as a function of temperature.

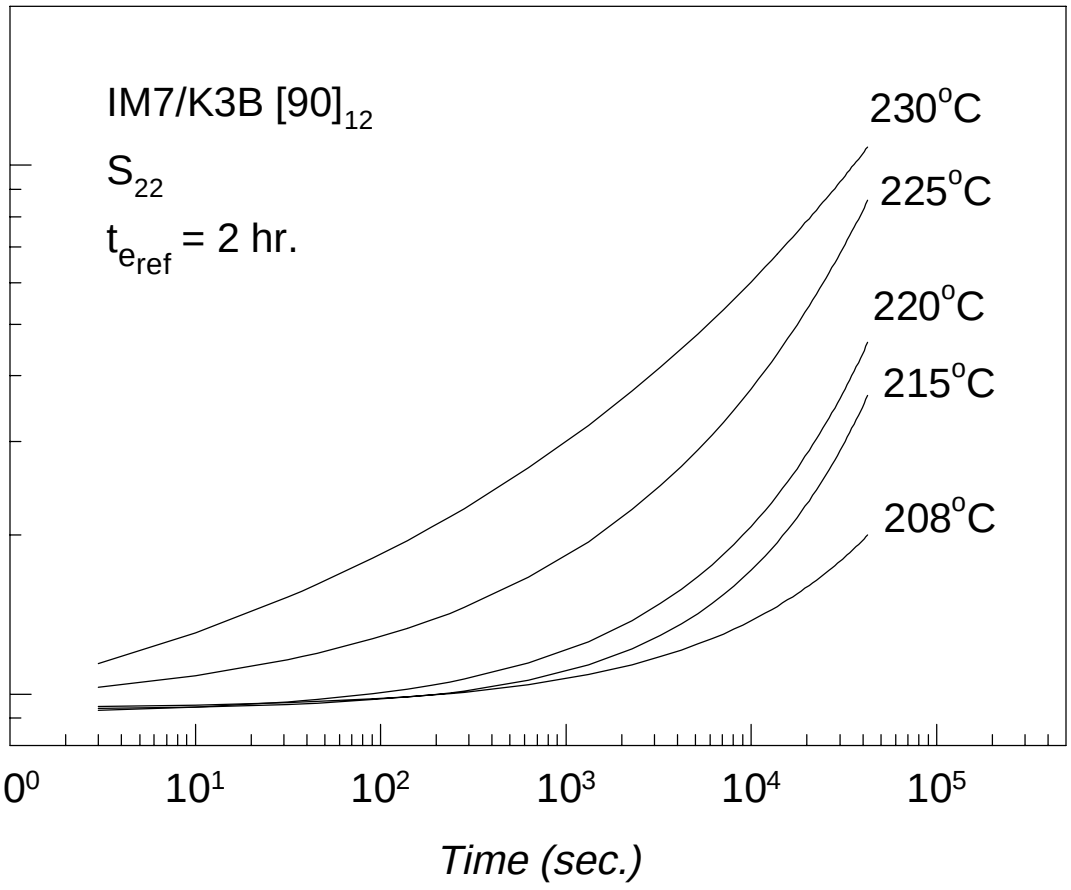

Fig. 13. Transverse compliance momentary master curves.

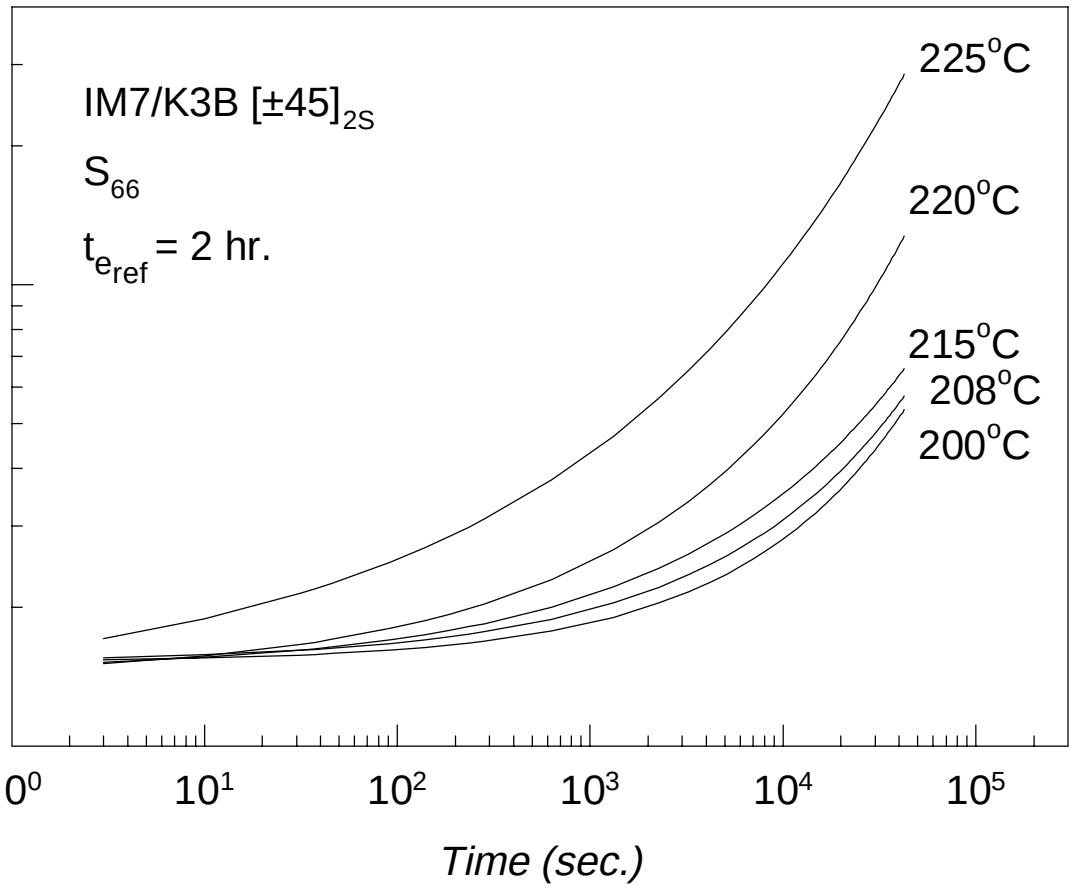

Fig. 14. Shear compliance momentary master curves.

Table 1. Momentary master curve parameters for both the transverse and shear creep compliance.

Compl. Terms	T (°C)	S_o (1/GPa)	τ (sec.)	β	μ	$\Delta\mu$ (Std. Dev.)
S_{22}	208	0.0937	7.76E+4	0.468	0.808	0.0827
S_{22}	215	0.0933	2.43E+4	0.559	0.742	0.0327
S_{22}	220	0.0914	1.53E+4	0.470	0.751	0.0370
S_{22}	225	0.0923	3378.87	0.316	0.644	0.0579
S_{22}	230	0.0589	43.617	0.155	0.587	0.0155
S_{66}	200	0.1521	2.68E+4	0.497	0.857	0.0356
S_{66}	208	0.1521	2.21E+4	0.433	0.871	0.0089
S_{66}	215	0.1452	1.39E+4	0.368	0.853	0.0071
S_{66}	220	0.1402	4595.7	0.356	0.791	0.0510
S_{66}	225	0.1297	485.60	0.252	0.574	0.0603